

OUT-4102-60  
UTAS-PHYS-95-40  
MZ-TH/95-22  
hep-ph/9509296  
September, 1995

## Unknotting the polarized vacuum of quenched QED<sup>\*)</sup>

**D. J. Broadhurst**<sup>1)</sup>

Physics Department, Open University  
Milton Keynes MK7 6AA, United Kingdom

**R. Delbourgo**<sup>2)</sup>

Department of Physics, University of Tasmania  
GPO Box 252C, Hobart, Tasmania 7001, Australia

**D. Kreimer**<sup>3)</sup>

Institut für Physik, Johannes Gutenberg-Universität  
Postfach 3980, D-55099 Mainz, Germany

**Abstract** A knot-theoretic explanation is given for the rationality of the quenched QED beta function. At the link level, the Ward identity entails cancellation of subdivergences generated by one term of the skein relation, which in turn implies cancellation of knots generated by the other term. In consequence, each bare three-loop diagram has a rational Laurent expansion in the Landau gauge, as is verified by explicit computation. Comparable simplification is found to occur in scalar electrodynamics, when computed in the Duffin-Kemmer-Petiau formalism.

---

<sup>\*)</sup> Work supported in part by grant CHRX-CT94-0579, from HUCAM, and grant A69231484, from the Australian Research Council.

<sup>1)</sup> D.Broadhurst@open.ac.uk

<sup>2)</sup> Delbourgo@physvax.phys.utas.edu.au

<sup>3)</sup> Kreimer@dipmza.physik.uni-mainz.de

**1. Introduction** The surprising rationality of the three- [1] and four-loop [2] quenched (i.e. single-electron-loop) terms in the QED beta function is an outstanding puzzle, which we here elucidate by giving the Ward identity  $Z_1 = Z_2$  an interpretation in terms of the skeining relation that is the basis of the recent association of knots [3, 4, 5, 6] with transcendental counterterms.

In Section 2, we study the intricate cancellations between transcendentals in all 6 of the methods (known to us) for calculating  $\beta(a) \equiv da/d\ln\mu^2 = \sum_n \beta_n a^{n+1}$ , with a QED coupling  $a \equiv \alpha/4\pi$ . Our focus is the rationality of  $\beta_3^{[1]} = -2$  [1] and  $\beta_4^{[1]} = -46$  [2]. (Subscripts denote the number of loops; where necessary, superscripts denote the number of electron loops.) In Section 3, we compound the puzzle by exposing even more intricate cancellations of  $\zeta_3$  in three-loop scalar electrodynamics [7]. The argument from knot theory is given in Section 4, leading to specific predictions, confirmed by detailed calculations, performed using the techniques of [8, 9, 10]. Conclusions, regarding higher orders [2], unquenched (i.e. multi-electron-loop) contributions [11, 12, 13], and non-abelian gauge theories [14, 15], are presented in Section 5.

**2. Six calculations in search of an argument** There are (at least) 6 ways of obtaining the beta function of quenched QED. For each, we expose the delicate cancellation of transcendentals between diagrams, which cries out for explanation.

*Method 1: Dyson-Schwinger skeleton expansion* [1, 16]. The Dyson-Schwinger equations give the photon self-energy, schematically, as [17]

$$\Pi_{\mu\nu} = Z_1 \Gamma_\mu G \gamma_\nu = \Gamma_\mu G (1 - KG) \Gamma_\nu, \quad (1)$$

where  $\Gamma_\mu$  is the dressed vertex and  $G$  stands for the pair of dressed propagators in Fig. 1a. To obtain the second form, illustrated in Figs. 1b,c, one uses  $\Gamma_\nu = Z_1 \gamma_\nu + KG \Gamma_\nu$ , where  $K$  is the kernel for  $e^+e^-$  scattering and loop integrations and spin sums are to be understood in the products. Now we expand each vertex to first order in the external momentum  $q$ :  $\Gamma_\mu = \Gamma_\mu^0 + q \cdot d\Gamma_\mu + O(q^2)$  where  $d_\alpha \equiv \partial/\partial q_\alpha$  and the Ward identity gives  $\Gamma_\mu^0 \equiv \Gamma_\mu(p, p) = (\partial/\partial p_\mu) S^{-1}(p)$  in term of the inverse propagator. We use the low-momentum expansion

$$(\Gamma_\mu - \Gamma_\mu^0)G(1 - KG)(\Gamma_\nu - \Gamma_\nu^0) = (q \cdot d\Gamma_\mu)G(1 - KG)(q \cdot d\Gamma_\nu) + O(q^3), \quad (2)$$

differentiate twice, and make liberal use of  $(1 - KG)d_\alpha \Gamma_\nu = d_\alpha(KG)\Gamma_\nu^0 + O(q)$ , to obtain

$$\begin{aligned} d_\alpha d_\beta \Pi_{\mu\nu} &= \Gamma_\mu^0 \left[ \frac{1}{2} d_\alpha d_\beta G + (d_\alpha G)K(d_\beta G) + 2(d_\alpha G)(d_\beta K)G + \frac{1}{2}G(d_\alpha d_\beta K)G \right. \\ &\quad \left. + (d_\alpha(GK))G(1 - KG)^{-1}(d_\beta(KG)) + (\alpha \leftrightarrow \beta) \right] \Gamma_\nu^0 + O(q), \end{aligned} \quad (3)$$

which entails only  $K$  and  $S$ . There is a very simple statement of this result: between the dressed zero-momentum vertices occur all and only the terms in  $d_\alpha d_\beta (G(1 - KG)^{-1})$  that give no subdivergences. In other words, the Dyson-Schwinger method kills maximal forests of subdivergences both on the left and on the right; only the overall divergence survives. Moreover, after cutting at a line on the left (or right), we may set both the mass and the external momentum to zero, with no danger of infrared divergence, and hence obtain the  $L$ -loop quenched beta function from finite massless two-point skeleton diagrams, with up to  $(L - 1)$ -loops.

We route half of the external momentum through the electron line and half through the positron line and find that each of the 5 terms in (3) yields a contraction-independent

contribution to  $\beta_3^{[1]}$ . To all orders, the first contribution to  $\beta^{[1]}(a)$  is  $\frac{4}{3}a^2(1 - \frac{3}{2}\gamma^2 + \gamma^3)$ , where  $\gamma \equiv \gamma_2^{[0]} = \xi a - \frac{3}{2}a^2 + \frac{3}{2}a^3 + O(a^4)$ , is the quenched electron-field anomalous dimension [18] with a photon propagator  $g_{\mu\nu}/k^2 + (\xi - 1)k_\mu k_\nu/k^4$ . The second term gives  $\beta_2 = 4$ . At 3 loops, all 5 terms contribute, giving a remarkable cancellation of  $\zeta_3$ :

$$\begin{aligned} \beta_3^{[1]} = & -2\xi^2 + \left[ -\frac{2}{3}(7\xi - 3)(\xi - 3) + 2(\xi^2 - 6\xi - 3)\zeta_3 \right] + (\xi - 1)(\xi - 5) \left[ \frac{16}{3} - 4\zeta_3 \right] \\ & + \left[ \frac{4}{3}(\xi^2 + 12\xi - 23) + 2(\xi^2 - 6\xi + 13)\zeta_3 \right] + 8 = -2. \end{aligned} \quad (4)$$

In the Landau gauge,  $\xi = 0$ , we reproduce Rosner's  $\zeta_3$ -cancellation:  $0 = -6 - 20 + 26$  [1]. In the Feynman gauge,  $\xi = 1$ , the third term vanishes; the second and fourth are still transcendental and exactly cancel the fifth.

*Method 2: Integration by parts of massive bubble diagrams* [8]. We may study separately each of the 3-loop quenched diagrams of Fig. 2, using the techniques of [8], which reduce to algebra the calculation of 3-loop massive bubble diagrams, in  $d \equiv 4 - 2\epsilon$  dimensions, thereby also yielding the finite parts of on-shell charge renormalization, used in [10] to establish the connection between 4-loop on-shell and minimally subtracted (unquenched) beta functions. The coefficient,  $d_n$ , of  $a^n/\epsilon$ , in the sum of all  $n$ -loop, single-electron-loop, bare diagrams contributing to  $1/Z_3$ , differs from  $\beta_n^{[1]}/n$ ; one must also take account of the quenched anomalous mass dimension,  $\gamma_m^{[0]} = \sum_n \gamma_n a^n = 3a + \frac{3}{2}a^2 + \frac{129}{2}a^3 + O(a^4)$  [18]. To 4 loops, the effects of mass renormalization are also rational, giving agreement with 3-loop results [8, 10]:

$$d_1 = \beta_1 = \frac{4}{3}; \quad d_2 = \frac{1}{2}\beta_2 - 2\beta_1\gamma_1 = -6; \quad d_3 = \frac{1}{3}\beta_3^{[1]} - 2\beta_2\gamma_1 - \beta_1\gamma_2 + 6\beta_1\gamma_1^2 = \frac{136}{3}; \quad (5)$$

and generating a 4-digit prime in the quenched 4-loop coefficient:

$$d_4 = \frac{1}{4}\beta_4^{[1]} - 2\beta_3^{[1]}\gamma_1 - \beta_2\gamma_2 + 8\beta_2\gamma_1^2 + 8\beta_1\gamma_2\gamma_1 - \frac{2}{3}\beta_1\gamma_3 - \frac{64}{3}\beta_1\gamma_1^3 = -\frac{2969}{6}, \quad (6)$$

which string-inspired techniques [19] may eventually reproduce. In the simplest case [8] of contracting  $d_\alpha d_\beta \Pi_{\mu\nu}|_{q=0}$  with  $g_{\mu\nu}g_{\alpha\beta}$  in the Feynman gauge, we find cancelling coefficients of  $\zeta_3/\epsilon$  in the contributions of Figs. 2f and 2g, corresponding to  $\zeta_3$ -cancellation between the fourth and second terms, respectively, of (4) at  $\xi = 1$ .

*Method 3: Integration by parts of massless two-point diagrams* [20, 21]. Next we study the behaviour of the bare diagrams of Fig. 2 at large  $q^2$  [21], where we may set  $m = 0$  and have no need of mass renormalization, or differentiation. The integration-by-parts method of Chetyrkin and Tkachov [20] now suffices. It has been implemented in the program MINCER, whose test suite [22] evaluates all the diagrams of Fig. 2 in the Feynman gauge. Table 1 of [22] reveals that, in addition to the crossed-photon diagrams of Fig. 2f and 2g, the uncrossed-photon diagrams of Figs. 2a and 2e also entail  $\zeta_3/\epsilon$ . Moreover, the cancellation does not occur in the crossed and uncrossed sectors separately; the relative weights of  $\zeta_3/\epsilon$  in the contributions of the bare diagrams 2a,e,f,g are  $3 : -6 : -1 : 4$ .

*Method 4: Infrared rearrangement of massless diagrams* [14, 23, 24]. Infrared rearrangement is a technique for reducing the calculation of  $L$ -loop counterterms to that of  $(L - 1)$ -loop massless two-point diagrams, by the subtraction of subdivergences in the MS scheme, followed by nullification of external momenta and appropriate cutting of massless

bubble diagrams. As shown by Method 1, the Dyson-Schwinger equations make this unnecessary in QED. However, the technique prospered at the 3-loop level in QCD [14, 23] to such an extent as to encourage the calculation of the 4-loop beta function of QED, with the rational quenched result  $\beta_4^{[1]} = -46$  [2]. A measure of the seemingly miraculous cancellation of transcendentals in this method is afforded by the complicated combination of  $\zeta_3$  and  $\zeta_5$  that occurs in the *non*-abelian 4-loop QCD corrections to  $R(e^+e^- \rightarrow \text{hadrons})$  [25].

*Method 5: Propagation in a background field* [26, 27]. As observed in [26], the derivative  $(d/da)(\beta^{[1]}(a)/a^2) = \sum_{n>1} (n-1)\beta_n^{[1]}a^{n-2}$  may be obtained from the coefficient of  $\alpha F_{\mu\nu}^2$  in the single-electron-loop contributions to the large- $q^2$  photon propagator in a background field  $F_{\mu\nu}$ , thereby providing a further alternative to infrared rearrangement. Two-loop massless background-field calculations have been performed in QCD [27, 28], with results recently confirmed by a full analysis of the massive case [29]. From the two-loop corrections,  $1 + (2C_A - C_F)\alpha_s/4\pi$ , to the coefficient of  $\langle \alpha_s G_{\mu\nu}^2 \rangle$  in the correlator of the light-quark vector current of QCD, one immediately obtains  $2\beta_3^{[1]}/\beta_2 = -1$ , by setting  $C_A = 0$ ,  $C_F = 1$ , which confirms the correctness of this method at 3 loops. A measure of the complexity of the  $\zeta_3$  cancellations is afforded by studying the diagram-by-diagram analysis of the appendix of [28].

*Method 6: Crewther connection to deep-inelastic processes* [30, 31]. Finally, a useful check of  $\beta_4^{[1]} = -46$  was obtained in [30] by taking the reciprocal of the 3-loop [31] radiative corrections to the Gross-Llewellyn-Smith sum rule, in the quenched abelian case:

$$\beta^{[1]}(a) = \frac{\frac{4}{3}a^2}{1 - 3a + \frac{21}{2}a^2 - \frac{3}{2}a^3 + O(a^4)} = \frac{4}{3}a^2 + 4a^3 - 2a^4 - 46a^5 + O(a^6), \quad (7)$$

in precise agreement with [2]. This is an example of a Crewther connection [32] which is unmodified by renormalization in quenched QED. A measure of the complexity of the cancellations of  $\zeta_3$  and  $\zeta_5$  is afforded by studying the *non*-abelian terms in 3-loop deep-inelastic radiative corrections [31], which are replete with both transcendentals.

**3. Cancellation of  $\zeta_3$  in scalar electrodynamics** Corresponding calculations in scalar electrodynamics (SED) are most conveniently performed using the Duffin-Kemmer-Petiau [33] (DKP) spinorial formalism for the charged scalar field, in which the Feynman rules are identical to those of fermionic QED, with a bare vertex  $e_0\gamma_\mu$  and a bare propagator  $S_0(p) = 1/(\not{p} - m_0)$ . The only difference resides in the  $\gamma$ -matrices: in the DKP formalism  $\not{p}$  is not invertible; instead one uses the fact that  $\not{p}^3 = p^2\not{p}$  to obtain  $S_0(p) = (\not{p}(\not{p} + m_0)/(p^2 - m_0^2) - 1)/m_0$ . The trace of the unit matrix is  $d + 1$ , the trace of an odd number of  $\gamma$ -matrices vanishes, and the trace of an even number,  $\gamma_{\mu_1}$  to  $\gamma_{\mu_{2n}}$ , is the sum of two terms [34]:  $g_{\mu_1\mu_2} \dots g_{\mu_{2n-1}\mu_{2n}}$  and the cyclic permutation  $g_{\mu_2\mu_3} \dots g_{\mu_{2n}\mu_1}$ . The effect is to make all traces regular as  $m_0 \rightarrow 0$ , while automatically generating the many seagull terms of conventional scalar methods [17]. This is a great simplification, eliminating the need to include 21 seagull diagrams at 3 loops, which would lead to many more terms in  $d_\alpha d_\beta \Pi_{\mu\nu}|_{q=0}$ .

We compute the diagrams of Fig. 2 using the DKP formalism. At  $q = 0$  (Method 2) we use the REDUCE [35] program RECURSOR [8], for 3-loop massive bubble diagrams; at  $m = 0$ , we use the REDUCE program SLICER [10], devised to check the results of [21] for the large- $q^2$  photon propagator in the  $\overline{\text{MS}}$  scheme. As in QED, we perform both calculations in an arbitrary gauge and contract  $d_\alpha d_\beta \Pi_{\mu\nu}$  with  $g_{\mu\nu}g_{\alpha\beta} + \lambda(g_{\mu\nu}g_{\alpha\beta} + g_{\mu\alpha}g_{\nu\beta} + g_{\nu\alpha}g_{\mu\beta})$ ,

where  $\lambda$  is an arbitrary parameter, which affects the contributions of individual diagrams, but not the total result for the transverse self energy  $\Pi_{\mu\nu}(q) = (q_\mu q_\nu - q^2 g_{\mu\nu})\Pi(q^2)$ . At  $m = 0$ , the corresponding freedom is to contract with the tensor  $g_{\mu\nu}q^2 + \lambda(d+2)q_\mu q_\nu$ . On-shell SED mass renormalization is performed as in [8, 9]: there are only two quenched self-energy diagrams at two loops; each is projected on-shell by taking the trace with  $\not{p}(\not{p} + m)$  at  $p^2 = m^2$ , with a pole mass  $m$ . Unlike the QED case, the relation between bare and pole masses is infrared-singular in SED, though that causes no problem for the dimensionally regularized calculation of  $Z_3 = 1/(1 + \Pi_0(0))$ , where infrared singularities in the bare diagrams for  $\Pi_0(0)$  are cancelled by those in  $Z_m \equiv m_0/m$ . The on-shell methods of [8] then yield the quenched contributions

$$\frac{1}{Z_3^{[1]}} - 1 = \begin{cases} \frac{4}{3\epsilon} a_m + \frac{4(1+7\epsilon-4\epsilon^3)}{\epsilon(2-\epsilon)(1-4\epsilon^2)} a_m^2 + \left[ -\frac{2}{3\epsilon} + 16\zeta_2(5 - 8 \ln 2) + \frac{1}{3}\zeta_3 + \frac{77}{9} \right] a_m^3, \\ \frac{1}{3\epsilon} a_m + \frac{4}{\epsilon(2-\epsilon)(1-4\epsilon^2)} a_m^2 + \left[ +\frac{29}{6\epsilon} + 8\zeta_2(3 - 4 \ln 2) + \frac{35}{12}\zeta_3 + \frac{136}{9} \right] a_m^3, \end{cases} \quad (8)$$

for QED [8, 10] and SED, respectively, where  $a_m = \Gamma(1+\epsilon)e_0^2/(4\pi)^{d/2}m^{2\epsilon}$  is a dimensionless coupling, with a pole mass  $m$ , and terms of order  $a_m^3\epsilon$  and  $a_m^4$  are neglected. (There is no need to renormalize the bare charge,  $e_0$ , when dealing with the quenched contributions.) From the singular terms in (8) we read off the 3-loop beta function of quenched SED:  $\tilde{\beta}^{[1]}(a) = \frac{1}{3}a^2 + 4a^3 + \frac{29}{2}a^4 + O(a^5)$ . We have calculated the double-bubble term  $\tilde{\beta}_3^{[2]}$  in the on-shell and  $\overline{\text{MS}}$  schemes, obtaining agreement with [7] in the latter, as shown in Table 1.

For the 3-loop quenched  $\overline{\text{MS}}$  contributions to  $\Pi(q^2)$ , at large  $q^2$ , we obtain

$$\overline{\Pi}_3^{[1]}(q^2) = \begin{cases} \left[ -2 \ln(\mu^2/q^2) - \frac{286}{9} - \frac{296}{3}\zeta_3 + 160\zeta_5 \right] \bar{a}^3, \\ \left[ +\frac{29}{2} \ln(\mu^2/q^2) + \frac{502}{9} - \frac{160}{3}\zeta_3 + 40\zeta_5 \right] \bar{a}^3, \end{cases} \quad (9)$$

with  $\bar{a} = \Gamma(1+\epsilon)\Gamma^2(1-\epsilon)e_0^2/\Gamma(1-2\epsilon)(4\pi)^{d/2}\mu^{2\epsilon}$ , which suppresses  $\zeta_2$  in Laurent expansions. The QED result confirms [21]. The SED cancellations are even subtler: with  $\xi = \lambda = 0$  the relative weights of  $\zeta_3/\epsilon$  from bare diagrams 2a,e,f,g,h are 18 : -36 : -5 : 22 : 1.

**4. The argument from knot theory** From the point of view of knot theory, as proposed in [3, 4, 5, 6], the presence of transcendentals in counterterms can be traced to the knots that are obtained by skeining the link diagrams that encode the intertwining of loop momenta in Feynman diagrams. The absence of transcendentals in the quenched beta function does not, therefore, correspond to the absence of knots in the Feynman graphs, since the crossed-photon graphs of Figs. 2f,g,h all realize the link diagram whose skeining contains the trefoil knot [4]. Accordingly we expect to find  $\zeta_3/\epsilon$  in their divergent parts. To explain the cancellation of transcendentals, we must study the interplay between knot-theoretic arguments and the gauge structure of QED.

It was found in [3, 4] that ladder topologies are free of transcendentals when the appropriate counterterms are added: after minimal subtraction of subdivergences, ladder graphs, such as in Figs. 2a,e, give rational terms in the Laurent expansion in powers of  $1/\epsilon$ . In [5, 6], on the other hand, transcendentals corresponding to positive knots, with up to 11 crossings, were successfully associated with subdivergence-free graphs, up to 7 loops. Thus the skein relation played two distinct roles in previous applications: in [3] the so-called  $A$  part of the skein operation determined the subdivergences, while the  $B$  part gave no non-trivial knots in ladder topologies; in [5] there were no subdivergences associated with the  $A$  operation, while the knots from the  $B$  operation faithfully revealed

the transcendentals resulting from nested subintegrations. In Figs. 2f,g,h we are now confronted with Feynman diagrams whose link diagrams generate the trefoil knot (via  $B$ ) and also have subdivergences (corresponding to  $A$ ).

We thus propose to associate the cancellation of transcendentals with the cancellation of subdivergences in the quenched beta function of QED, which is an immediate consequence of the Ward identity,  $Z_1 = Z_2$ .

To see the key role of the Ward identity, consider Fig. 2g. There is an internal vertex correction, which is rendered local by adding the appropriate counterterm graph. Due to the Ward identity, this counterterm graph is the same as that which compensates for the self-energy correction in Fig. 2e. In [3, 4] it was shown that the latter counterterm could be interpreted as the  $A$  part of the skein operation on the link diagram  $L(2e)$  of Fig. 3, associated with the Feynman graph 2e. We assume that this is a generic feature of the relationship between skeining and renormalization and associate the corresponding counterterm for Feynman graph 2g with the term obtained from applying  $A$  twice to the link diagram  $L(2g)$ , which requires two skeinings to generate the same counterterm, along with the trefoil knot from the  $B$  term. The Ward identity thus becomes a relation between crossed and uncrossed diagrams, after skeining:

$$A(A(L(2g))) = A(L(2e)) \quad \Rightarrow \quad A(L(2g)) = L(2e). \quad (10)$$

The trefoil knot results, in this language, from  $B(B(L(2g)))$ , which generates, in general, a  $\zeta_3/\epsilon$  term from Fig. 2g, even after the subtraction of subdivergences. We now use the Ward identity (10) at the link level to obtain

$$B(B(L(2g))) = B(B(A^{-1}(L(2e)))) , \quad (11)$$

from which we see that it relates the transcendental counterterm from a torus-knot [4] topology, in Fig. 2g, to a knot-free [3] ladder topology, in Fig. 2e.

We conclude that  $\zeta_3/\epsilon$  should be absent from the bare diagram of Fig. 2g when it is calculated in the gauge where the bare diagram of Fig. 2e is free of  $\zeta_3/\epsilon$ , i.e. in the Landau gauge, where the latter is free of subdivergences. In Fig. 3 we summarize the argument. By a similar argument, we also conclude that the other graphs with the trefoil topology, namely Figs. 2f,h, should be free of  $\zeta_3/\epsilon$  in the Landau gauge.

Note that vanishing of the bare ladder diagram of Fig. 2e, in the Landau gauge, does not imply the vanishing of  $B(B(A^{-1}(L(2e))))$ ; it merely implies its rationality. The action of the  $A$  and  $B$  operators is non-trivial on the diagram of Fig. 2e; in the language of [3, 4], skeining involves a change of writhe number in the subdivergence, and only terms with writhe number zero vanish in the Landau gauge, while the double application of the  $B$  operator in  $B(B(A^{-1}(L(2e))))$  generates a non-vanishing writhe for the subdivergence.

To test these ideas, we evaluate the separate contributions of the QED diagrams of Fig. 2 to (8,9) in the Landau gauge and find, indeed, that *each* bare diagram has a rational  $1/\epsilon$  term in its Laurent expansion, at  $\xi = 0$ , for any value of the contraction parameter,  $\lambda$ . In any other gauge, the bare massless diagrams of Figs 2a,e,f,g give non-zero, mutually cancelling, coefficients of  $\zeta_3/\epsilon$ . The  $m = 0$  contributions to the Laurent expansion of  $\Pi_3^{[1]}$  are given in Table 2, in the case  $\xi = \lambda = 0$ . The same rational behaviour is observed in the Landau gauge at  $q = 0$  (again for any value of  $\lambda$ ) with contributions also recorded in Table 2 (with  $\lambda = 0$ ), along with that from mass renormalization of lower-loop diagrams.

To determine the corresponding gauge for SED, we study both of the two-loop DKP diagrams and find that each gives  $1/\epsilon^2$  terms, proportional to  $2\xi - 3$ . Thus the gauge  $\xi = 3/2$  is the closest DKP analogy to the Landau gauge of QED. In any gauge, however, diagram 2h gives a  $\zeta_3/\epsilon$  term, proportional to  $\lambda - 2$ . (The absence of such a term in QED is attributable to the fact that the finite part of the two-loop fermion propagator does not involve  $\zeta_3$  at large momentum.) Accordingly we evaluate all  $m = 0$  and  $q = 0$  SED diagrams with  $\xi = 3/2$  and  $\lambda = 2$  and find that every one is indeed rational, with a Laurent expansion recorded in Table 3. Again, we regard this as a significant success of skeining arguments, since fixing 2 parameters removes  $\zeta_3/\epsilon$  from each of the 5 diagrams 2a,e,f,g,h.

**5. Conclusions** Complete cancellation of transcendentals from the beta function, at every order, is to be expected only in quenched QED and quenched SED, where subdivergences cancel between bare diagrams.

Contributions with more than one charged loop require scheme-dependent coupling-constant renormalization. Knot theory guarantees that double-bubble contributions are rational at the three-loop level, as found in [7, 11] and shown in Table 1. But at four loops [2, 10, 12], and beyond [13], such multi-electron-loop contributions entail non-trivial knots, associated with zeta functions [4] and more exotic [5, 6] transcendentals, whose cancellation is *not* underwritten by the Ward identity.

Likewise, we do not expect the beta functions of *non*-abelian gauge theories to be rational beyond the presently computed [14, 15] three-loop level, since coupling-constant renormalization is required to remove subdivergences generated by gluon- and ghost-loops in the gluon self-energy, which cannot be quenched without violating the Slavnov-Taylor identities. Indeed, it is still somewhat obscure how the rationality of  $\beta_3$  comes about in QCD: as shown in [15], the renormalization constants  $Z_{1,2,3}$ , for the quark-gluon vertex, quark field, and gluon field, all involve  $\zeta_3/\epsilon$  at three-loops; only in  $Z_\alpha = Z_1^2 Z_2^{-2} Z_3^{-1}$  does the cancellation occur. It may be possible to understand this in a three-loop background-field calculation, but we do not expect the intrinsically scheme-dependent non-abelian beta function to remain rational at higher orders in the  $\overline{\text{MS}}$  scheme.

In fact, there are only two further quantities that we expect to be rational beyond three loops: the quenched anomalous field and mass dimensions,  $\gamma_2^{[0]}$  and  $\gamma_m^{[0]}$ , of QED, whose rationality at the three-loop level is established in [15, 18]. These are scheme-independent, since subdivergences cancel in the electron propagator, by virtue of the Ward identity, which here relates proper self-energy diagrams to one-particle-reducible diagrams.

One is tempted to seek a calculational method, based on the skein relation, to compute the rational anomalous dimensions of quenched QED, in terms of diagrams, with non-zero writhe numbers, that have been ‘ladderized’ by Ward identities, such as (11), which may eventually yield a rational calculus like that in [4]. The complexity of the rational contributions of Tables 2 and 3 indicates that such a calculus would be rather non-trivial.

In conclusion: all-order rationality of counterterms is specific to quenched abelian theories, where the cancellation of knots, from the  $B$  term [5, 6] in the skein relation, matches the cancellation of subdivergences, from the  $A$  term [3, 4]. This is exemplified by the rationality of all quenched three-loop bare QED diagrams, in the Landau gauge.

**Acknowledgements** DJB and DK thank the organizers and participants of the Pisa and Aspen multi-loop workshops for their interest in and comments on this work. Detailed discussions with Kostja Chetyrkin, John Gracey, Sergei Larin, Christian Schubert and Volodya Smirnov were most helpful. DJB thanks Andrei Kataev and Eduardo de Rafael, for long-standing dialogues on the rationality of quenched QED, and the organizers of the UK HEP Institute in Swansea, where the computations were completed.

## References

- [1] J.L. Rosner, Phys. Rev. Lett. **17** (1966) 1190; Ann. Phys. **44** (1967) 11.
- [2] S.G. Gorishny, A.L. Kataev, S.A. Larin and L.R. Surguladze, Phys. Lett. **B256** (1991) 81.
- [3] D. Kreimer, Renormalization and Knot Theory, UTAS-PHYS-94-25, to appear in Journal of Knot Theory and its Ramifications.
- [4] D. Kreimer, Phys. Lett. **B354** (1995) 117.
- [5] D.J. Broadhurst and D. Kreimer, Knots and numbers in  $\phi^4$  theory to 7 loops and beyond, OUT-4102-57, hep-ph/9504352, to appear in New Computing Techniques in Physics Research IV (World Scientific, in press).
- [6] D.J. Broadhurst and D. Kreimer, Systematic identification of transcendental counterterms with positive knots, OUT-4102-61, in preparation.
- [7] K.G. Chetyrkin, S.G. Gorishny, A.L. Kataev, S.A. Larin and F.V. Tkachov, Phys. Lett. **B116** (1982) 455.
- [8] D.J. Broadhurst, Z. Phys. **C54** (1992) 599.
- [9] N. Gray, D.J. Broadhurst, W. Grafe and K. Schilcher, Z. Phys. **C48** (1990) 673; D.J. Broadhurst, N. Gray and K. Schilcher, Z. Phys. **C52** (1991) 111.
- [10] D.J. Broadhurst, A.L. Kataev and O.V. Tarasov, Phys. Lett. **B298** (1993) 445.
- [11] E. de Rafael and J.L. Rosner, Ann. Phys. **82** (1974) 369.
- [12] T. Kinoshita, H. Kawai and Y. Okamoto, Phys. Lett. **B254** (1991) 235; H. Kawai, T. Kinoshita and Y. Okamoto, Phys. Lett. **B260** (1991) 193; A.L. Kataev, Phys. Lett. **B284** (1992) 401.
- [13] A. Palanques-Mestre and P. Pascual, Comm. Math. Phys. **95** (1984) 277; J.A. Gracey, Mod. Phys. Lett. **A7** (1992) 1945; D.J. Broadhurst, Z. Phys. **C58** (1993) 339.
- [14] O.V. Tarasov, A.A. Vladimirov and A.Y. Zharkov, Phys. Lett. **B93** (1980) 429.
- [15] S.A. Larin and J.A.M. Vermaseren, Phys. Lett. **B303** (1993) 334.
- [16] K. Johnson, R. Willey and M. Baker, Phys. Rev. **163** (1967) 1699.



- [17] J.D. Bjorken and S.D. Drell, *Relativistic Quantum Fields* (McGraw-Hill, 1965).
- [18] O.V. Tarasov, JINR P2-82-900 (1982);  
S.A. Larin, NIKHEF-H/92-18, hep-ph/9302240, in *Proc. int. Baksan School on Particles and Cosmology*, ed. E.N. Alexeev, V.A. Matveev, Kh.S. Nirov and V.A. Rubakov, (World Scientific, 1994).
- [19] M.G. Schmidt and C. Schubert, DESY 94-189; hep-th/9410100.
- [20] K.G. Chetyrkin and F.V. Tkachov, *Nucl. Phys.* **B192** (1981) 159;  
F.V. Tkachov, *Phys. Lett.* **B100** (1981) 65.
- [21] S.G. Gorishny, A.L. Kataev and S.A. Larin, *Phys. Lett.* **B273** (1991) 141;  
**B275** (1992) 512E; **B341** (1995) 448E.
- [22] S.G. Gorishny, S.A. Larin, L.R. Surguladze and F.V. Tkachov,  
*Comput. Phys. Commun.* **55** (1989) 381.
- [23] K.G. Chetyrkin, A.L. Kataev and F.V. Tkachov, *Phys. Lett.* **B85** (1979) 277;  
*Nucl. Phys.* **B174** (1980) 345.
- [24] K.G. Chetyrkin and F.V. Tkachov, *Phys. Lett.* **B114** (1982) 340.
- [25] S.G. Gorishny, A.L. Kataev and S.A. Larin, *Phys. Lett.* **B259** (1991) 144;  
*Pisma ZhETF* **53** (1991) 121.
- [26] K. Johnson and M. Baker, *Phys. Rev.* **D8** (1973) 1110.
- [27] K.G. Chetyrkin, S.G. Gorishny and V.P. Spiridonov, *Phys. Lett.* **B160** (1985) 149;  
G.T. Loladze, L.R. Surguladze and F.V. Tkachov, *Phys. Lett.* **B162** (1985) 363.
- [28] L.R. Surguladze and F.V. Tkachov, *Nucl. Phys.* **B331** (1990) 35.
- [29] D.J. Broadhurst, P.A. Baikov, V.A. Ilyin, J. Fleischer, O.V. Tarasov  
and V.A. Smirnov, *Phys. Lett.* **B329** (1994) 103;  
D.J. Broadhurst, J. Fleischer and O.V. Tarasov, *Z. Phys.* **C60** (1993) 287.
- [30] D.J. Broadhurst and A.L. Kataev, *Phys. Lett.* **B315** (1993) 179.
- [31] S.A. Larin and J.A.M. Vermaseren, *Phys. Lett.* **B259** (1991) 345.
- [32] R.J. Crewther, *Phys. Rev. Lett.* **28** (1972) 1421.
- [33] R.J. Duffin, *Phys. Rev.* **54** (1938) 1114;  
N. Kemmer, *Proc. R. Soc.* **166** (1938) 127; **A173** (1939) 91;  
G. Petiau, *Acad. R. Belg. Cl. Sci. Mem. Collect.* **16**(2) (1936);  
Z. Tokuoka and H. Tanaka, *Prog. Theor. Phys.* **8** (1952) 599;  
I. Fujiwara, *Prog. Theor. Phys.* **10** (1953) 589.
- [34] E. Fischbach, M.M Nieto and C.K. Scott, *J. Math. Phys.* **14** (1973) 1760.
- [35] A.C. Hearn, *REDUCE user's manual*, version 3.5, Rand publication CP78 (1993).

Table 1: Three-loop on-shell and MS coefficients of QED and SED beta functions.

$\beta_3^{[1]} + \beta_3^{[2]}$	QED	SED
on-shell	$-2 - \frac{224}{9} = -\frac{242}{9}$ [11]	$\frac{29}{2} - \frac{55}{18} = \frac{103}{9}$
MS	$-2 - \frac{44}{9} = -\frac{62}{9}$ [14]	$\frac{29}{2} - \frac{49}{18} = \frac{106}{9}$ [7]

Table 2: QED contributions to  $\Pi_3^{[1]}$ , at  $m = 0$  and  $q = 0$ , with  $\xi = \lambda = 0$ .

method	$m = 0$		$q = 0$	
	$\bar{a}^3/\epsilon^2$	$\bar{a}^3/\epsilon$	$a_m^3/\epsilon^2$	$a_m^3/\epsilon$
diagram 2a	0	8/3	0	8/3
diagram 2b	0	0	-12/5	152/5
diagram 2c	0	0	72/5	8/5
diagram 2d	0	0	2/3	31/3
diagram 2e	0	0	0	-24
diagram 2f	-2/3	7/3	-2/3	17/3
diagram 2g	0	-28/3	0	-28/3
diagram 2h	2/3	11/3	-12	28
uncrossed	0	8/3	38/3	21
crossed	0	-10/3	-38/3	73/3
mass renorm	0	0	0	-46
total	0	-2/3	0	-2/3

Table 3: SED contributions to  $\Pi_3^{[1]}$ , at  $m = 0$  and  $q = 0$ , with  $\xi = 3/2$  and  $\lambda = 2$ .

method	$m = 0$			$q = 0$		
	$\bar{a}^3/\epsilon^3$	$\bar{a}^3/\epsilon^2$	$\bar{a}^3/\epsilon$	$a_m^3/\epsilon^3$	$a_m^3/\epsilon^2$	$a_m^3/\epsilon$
diagram 2a	1/16	55/96	4151/576	1/16	7/96	2501/576
diagram 2b	-13/8	-409/24	-16243/144	-13/8	-233/120	-8/45
diagram 2c	3/2	31/2	3703/36	3/2	43/20	203/45
diagram 2d	1/16	103/96	4387/576	1/16	-65/96	-131/576
diagram 2e	0	-5/48	41/32	0	-5/48	-1141/96
diagram 2f	-1/16	-9/32	911/192	-1/16	7/32	1013/192
diagram 2g	0	3/16	-917/288	0	3/16	-1349/288
diagram 2h	1/16	3/32	-1667/576	1/16	-29/32	-809/576
uncrossed	0	0	37/6	0	-1/2	-55/16
crossed	0	0	-4/3	0	-1/2	-13/16
mass renorm	0	0	0	0	1	109/12
total	0	0	29/6	0	0	29/6

Fig. 1: Illustration of terms in the Dyson-Schwinger equation (1).

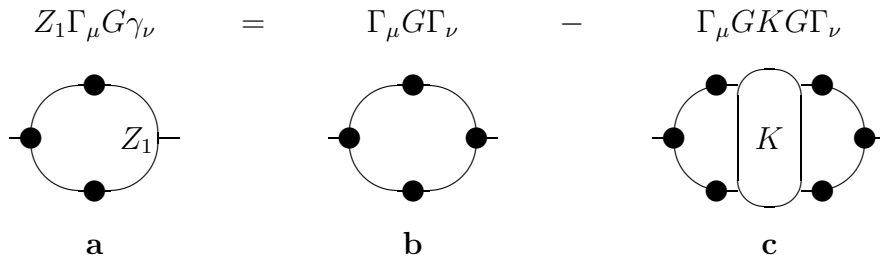


Fig 2: Diagrams contributing to  $\beta_3^{[1]}$ , with photon lines drawn inside the electron loop.

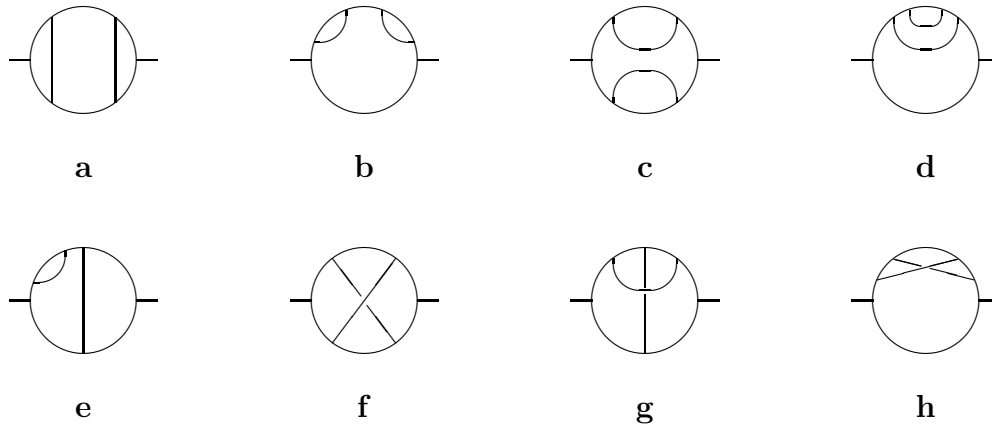


Fig. 3: The  $A$  part of the skein operation on the link diagrams for Figs. 2e,g.

